

Multi-gap superconductivity in a $\text{BaFe}_{1.84}\text{Co}_{0.16}\text{As}_2$ film from optical measurements at terahertz frequencies

A. Perucchi¹, L. Baldassarre¹, S. Lupi², J. Jiang³, J.D. Weiss³, E.E. Hellstrom³,
S. Lee⁴, C.W. Bark⁴, C.B. Eom⁴, M. Putti⁵, I. Pallecchi⁵, C. Marini⁶, P. Dore⁶

¹ *Sincrotrone Trieste S.C.p.A., S.S. 14 km 163.5,*

in Area Science Park, 34012 Basovizza (Trieste), Italy

² *CNR-IOM and Dipartimento di Fisica, Università di Roma Sapienza, P.le A.Moro 2, 00185 Rome, Italy*

³ *Applied Superconductivity Center, National High Magnetic Field Laboratory,
Florida State University, 2031 East Paul Dirac Drive, Tallahassee, FL 32310, USA*

⁴ *Department of Materials Science and Engineering,
University of Wisconsin-Madison, Madison, WI 53706, USA*

⁵ *CNR-SPIN and Dipartimento di Fisica, Università di Genova, Via Dodecaneso 33, 16146 Genova, Italy and*

⁶ *CNR-SPIN and Dipartimento di Fisica, Università di Roma "La Sapienza", P.le A.Moro 2, 00185 Rome, Italy*
(Dated: April 1, 2024)

We measured the THz reflectance properties of a high quality epitaxial thin film of the Fe-based superconductor $\text{BaFe}_{1.84}\text{Co}_{0.16}\text{As}_2$ with $T_c=22.5$ K. The film was grown by pulsed laser deposition on a DyScO_3 substrate with an epitaxial SrTiO_3 intermediate layer. The measured R_S/R_N spectrum, i.e. the reflectivity ratio between the superconducting and normal state reflectance, suggests the presence of a superconducting gap Δ_A close to 15 cm^{-1} . A detailed data analysis shows that a two-band, two-gap model is necessary to obtain a good description of the measured R_S/R_N spectrum. The low-energy Δ_A gap results to be well determined ($\Delta_A=15.5\pm0.5 \text{ cm}^{-1}$), while the value of the high-energy gap Δ_B is more uncertain ($\Delta_B=55\pm7 \text{ cm}^{-1}$). Our results provide evidence of two electronic contributions to the system conductivity with the presence of two optical gaps corresponding to $2\Delta/kT_c$ values close to 2 and 7.

PACS numbers: 74.78.-w, 74.25.Gz, 78.30.-j

I. INTRODUCTION

Since the early days of the discovery of superconductivity in the iron-pnictide family [1], analogies and differences with copper-oxide high- T_c superconductors have been extensively discussed. In particular, the importance of electron correlation [2] and the degree of itinerancy of the charge carriers [3] is still a matter of debate. Closely connected to that issue, is the problem of the symmetry of the superconducting order parameter. Indeed nodal gap symmetries are more liable to accommodate Cooper pairs in the presence of strong repulsions, than a fully gapped s -wave symmetry. Unfortunately, the determination of the gap properties of pnictides is further complicated by the fact that multiple bands are crossing the Fermi level, thus forming semi-metallic electron and hole pockets. While both nodal [4–7] and node-less [8–13] gaps have been proposed in literature, there is now a growing experimental evidence favouring the s -wave scenario. This finding is consistent with unconventional superconductivity mediated by spin-fluctuations, through the so-called s_{\pm} pairing state [14]. In this scenario, it is of basic importance a detailed knowledge of symmetry, number and values of the possible superconducting gaps.

In studying the superconducting Fe-based compounds, the 122 family obtained by doping of the parent compound AFe_2As_2 ($\text{A}=\text{Ba}, \text{Sr}, \text{Ca}$) is particularly suitable to explore the nature of the superconducting gaps, as it can be prepared in sizeable single crystals [15] as well as in high quality epitaxial thin films [16, 17]. Moreover,

compounds of the 122 phase are chemically and structurally simpler and more isotropic than those of the 1111 family (ReFeAsO , $\text{Re}=\text{rare earth}$), and can have a fairly high transition temperature. In particular, T_c can be as high as 25K in the electron doped $\text{BaFe}_{2-x}\text{Co}_x\text{As}_2$ compound [18], which is the object of the present work. The superconducting gaps in this system have been measured by various techniques, namely angle resolved photoemission spectroscopy (ARPES) [8], heat capacity [11], scanning tunneling spectroscopy [19, 20], penetration depth probed by μSR [10], point contact spectroscopy [9], Raman scattering [4], and thermal conductivity [12]. The results are widely scattered and even in sharp contrast with one another in terms of symmetry of the gaps, their number and their values. Indeed, the gaps have been found to be either nodal [4–7] or nodeless [8–13], isotropic [8, 9] or anisotropic [4, 12]. As to number and values of the gap(s), both a single gap [9, 19, 20] and two gaps [8, 10, 11, 13] have been reported in the range from $2\Delta/KT_c \simeq 2$ to $\simeq 7$. It is important to note that caution must be used in comparing results obtained on different samples since doping [8] and disorder [4, 12, 21, 22] have been indicated to be likely responsible for the apparent disagreement of literature data on gap values. Caution must be used also in comparing results obtained through different techniques since impurity effects, sample inhomogeneities, and surface off-stoichiometry can differently affect bulk and surface sensitive measurements.

In general, infrared spectroscopy is a powerful tool to study the properties of a conducting system since

the optical response of the free-charge carriers is determined by the frequency-dependent complex conductivity $\tilde{\sigma} = \sigma_1 + i\sigma_2$. In a simple one-band system, the standard Drude model (with parameters plasma frequency Ω and scattering rate γ) describes the complex conductivity $\tilde{\sigma}_N$ in the normal (N) state [23]. Here it is worth to recall that the *d.c.* conductivity $\sigma_0 = \sigma_1(\omega = 0)$ is proportional to Ω^2/γ . In the superconducting (S) state, the standard BCS model (Mattis-Bardeen equations [24], with parameters σ_0 and superconducting gap Δ) can describe the complex conductivity $\tilde{\sigma}_S$ [25]. On this basis, far-infrared/terahertz measurements can be of particular importance since a mark of the superconducting gap Δ can be observed at $\hbar\omega \sim 2\Delta$ (optical gap) for an isotropic *s*-wave BCS superconductor. For a bulk sample, in particular, a maximum at the optical gap is expected in the ratio R_S/R_N , where R_S and R_N are the frequency-dependent reflectances in the superconducting and normal state, respectively [25].

Infrared spectroscopy has been widely employed in studying Fe-based compounds [26, 27]. In particular, infrared/terahertz measurements on $\text{BaFe}_{2-x}\text{Co}_x\text{As}_2$ samples [28–34] have been recently employed to study the frequency dependent conductivity and to get information on the superconducting gap(s). However, there is still poor consensus on the value and, most importantly, on the number of gaps resulting from the analysis of THz data, as well as from the analysis of data from different techniques, as discussed above. In the present work we investigated the multiple-gap character of the Co-doped BaFe_2As_2 system by performing reflectance measurements at terahertz (THz) frequencies on a high quality film [16]. The results of the previous THz studies will be reported in the following, together with the results of the present work.

II. EXPERIMENTAL RESULTS

Epitaxial Co-doped BaFe_2As_2 films with high transition temperature were recently obtained by using novel template engineering [16]. The investigated 350 nm thick $\text{BaFe}_{1.84}\text{Co}_{0.16}\text{As}_2$ (BFCA) film was grown *in-situ* by using pulsed laser deposition (PLD) on an (110) oriented DyScO_3 (DSO) single crystal substrate with an intermediate layer (20 unit cell) of SrTiO_3 (STO). Out-of plane θ -2 θ X-ray diffraction was used to evaluate the quality and the orientation of the films: The full-width at half-maximum (FWHM) of the 004 rocking curve is indeed narrow (0.55°) and the 001 peaks, visible in the spectra, indicate that the film is grown with the *c*-axis normal to the substrate. For further informations on the film growth and on their epitaxial quality see Ref.[16].

The temperature-dependent resistivity $\rho(T)$ of the investigated film is reported in Fig.1, showing the onset of the superconducting transition at $T_c = 22.5$ K with a width of around 2 K. The error bar in the value of the residual resistivity ρ_0 ($0.15 \pm 0.01 \text{ m}\Omega\text{cm}$) is mainly due to

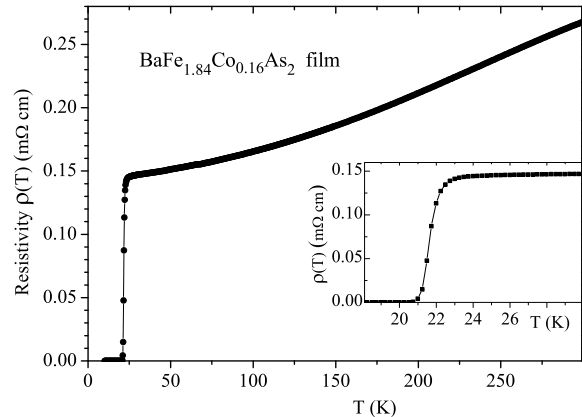


FIG. 1: (Color online) Resistivity $\rho(T)$ of the $\text{BaFe}_{0.84}\text{Co}_{0.16}\text{As}_2$ film. In the inset, a zoom of the superconducting transition. The residual resistivity is $\rho_0 = \rho(25 \text{ K}) = 0.15 \pm 0.01 \text{ m}\Omega\text{cm}$.

uncertainty in the film thickness t estimate ($350 \pm 25 \text{ nm}$).

We measured the $R(T)/R_N$ spectrum (where $R_N = R(25 \text{ K})$) of the BFCA film in the THz region by employing synchrotron radiation at the infrared beamline SISSI [35] at the synchrotron Elettra (Trieste, Italy). We remark that the large size of the film surface, together with the use of a high-flux synchrotron source, enables addressing the reflectivity at THz frequencies with superior signal to noise ratio with respect to measurements on single crystals. Indeed, our previous R_S/R_N measurements on an ultra-clean MgB_2 film, performed in the THz region by using synchrotron radiation, provided the first evidence of the effect of the two gaps in optical measurements [36], not observed in single crystals [37]. The $R(T)/R_N$ measurements were made by cycling the temperature in the 6–25 K range, without collecting reference spectra, in order to avoid any variation in the sample position and orientation, which may yield frequency-dependent systematic errors in $R(\omega)$. The obtained results are reported in Fig. 2a. We remark that the high accuracy of the present synchrotron measurements allows for the detection of small effects of the order of 0.1 % at THz frequencies.

For $T \simeq T_c$, the $R(T)/R_N$ curve is flat within experimental uncertainties, while on decreasing temperature the $R(T)/R_N$ spectrum increases on decreasing frequency until the R_S/R_N (with $R_S = R(6 \text{ K})$) reaches a plateau at about 30 cm^{-1} . At even lower frequencies, R_S/R_N becomes nearly constant. The frequency dependence of R_S/R_N first suggests the presence of a superconducting gap Δ close to 15 cm^{-1} . Indeed, for $\omega \rightarrow 0$, the reflectance R_N of a conducting system tends to 1 for a bulk system, and to a slightly lower value for a thin film, since the penetration depth becomes larger than the film thickness. Therefore, since R_S approaches 1 at $\omega = 2\Delta$,

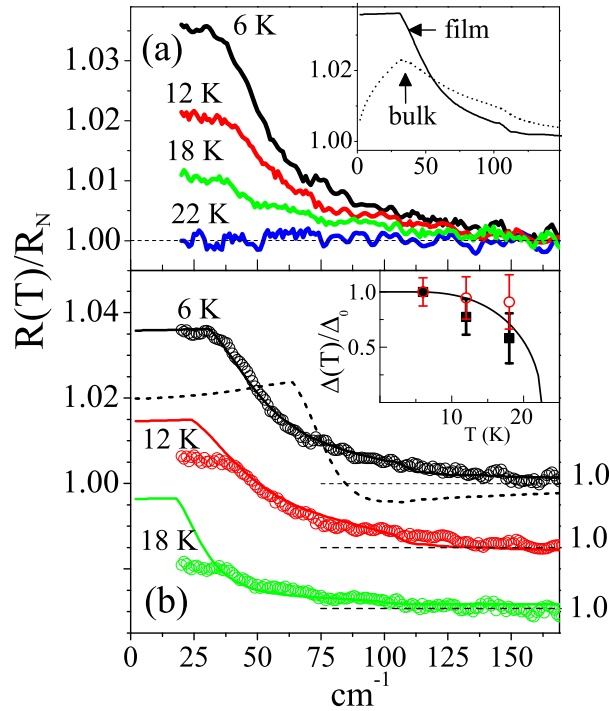


FIG. 2: (Color online)(a) $R(T)/R_N$ spectra of the BFCA film in the THz region. (b) The 6, 12, 18 K spectra conveniently shifted are compared with the two-band (full line) best fit profiles. In the 6 K case, also the one-band best fit profile (dotted line) is shown. In the inset of (a), the R/R_N best-fit model spectrum of the film is compared with the corresponding spectrum of a bulk sample (see text). In the inset of (b), the normalized $\Delta(T)/\Delta_0$ values are reported (Δ_A , full squares, Δ_B , open circles), with $\Delta_0 = \Delta(6 \text{ K})$. The full line is the standard BCS behaviour.

R_S/R_N exhibits a maximum around 2Δ in the case of a bulk sample, while it remains nearly constant below 2Δ in the film case[36].

III. ANALYSIS AND DISCUSSION

For a detailed analysis of the measured spectra, we used the procedure successfully employed in the MgB_2 [36] and V_3Si [38] cases. $\tilde{\sigma}_N$ is described by the Drude model, and $\tilde{\sigma}_S$ by the Zimmermann model [39] which generalizes the standard BCS model [24, 25] to arbitrary temperatures and to systems of arbitrary purity (i.e., to arbitrary γ values). $\tilde{\sigma}_S$ thus depends on the reduced temperature $t = T/T_c$ and on the parameters Ω , γ , and Δ . When two or more bands are assumed to contribute to the film conductivity, we employed the parallel conductivity model (in the two-band case [36, 37], $\tilde{\sigma} = \tilde{\sigma}_A + \tilde{\sigma}_B$), in both the normal and superconducting states.

From the calculated $\tilde{\sigma}$, by using standard relations [23],

it is then possible to compute the model refractive index $\tilde{n} = n + ik$ of the film. The reflectance spectrum of the three-layer system (film-STO-DSO) can then be evaluated by using the thickness and the n, k values of each layer [40]. For STO, detailed n and k values in the entire infrared region are reported in the literature [41]. Since such data are not available for DSO, we performed absolute reflectance measurements on a bare DSO substrate over a broad range, thus obtaining the n and k values relevant to this work. A detailed study of the DSO optical properties in the far-infrared region will be reported in a forthcoming paper. We verified that, for any reasonable choice of the Drude parameters determining n and k of the conducting film, the intermediate STO layer has no appreciable effect on the THz reflectance spectrum because of its extremely small thickness.

When only one band is supposed to contribute to the film conductivity (one-band, 1-b model), the unknown parameters which determine the R_S/R_N spectrum are Ω , γ , and Δ . We thus employed a three-parameters fitting procedure, and repeated the procedure for different values of the film thickness ($t = 350 \pm 25 \text{ nm}$). This procedure does not provide an at least satisfactory description of the R_S/R_N data independently of the t value, as shown by the best-fit curve in Fig. 2b, obtained for $t = 350 \text{ nm}$ with $\Omega = 3.2 \text{ eV}$, $\gamma = 800 \text{ cm}^{-1}$, and $\Delta = 32 \text{ cm}^{-1}$. The failure of the best fit profile in reproducing the experimental spectral shape, both above and below 2Δ , indicates the inadequacy of the 1-b model in describing the optical response of the film at THz frequencies.

In a two-band scenario, the six parameter ($\Omega_i, \gamma_i, \Delta_i, i = A, B$) fit provides a very good description of the R_S/R_N spectrum, as shown in Fig. 2b. We remark that only a two-band model can describe the measured R_S/R_N spectrum, and in particular the smoothly decreasing slope above 2Δ . The fit provides, for $t = 350 \text{ nm}$, plasma frequencies $\Omega_A \simeq 1 \text{ eV}$ and $\Omega_B \simeq 2 \text{ eV}$, $\gamma_A \simeq 200 \text{ cm}^{-1}$, $\gamma_B \simeq 2500 \text{ cm}^{-1}$, $\Delta_A \simeq 15 \text{ cm}^{-1}$, and $\Delta_B \simeq 55 \text{ cm}^{-1}$. The R_S/R_N best-fit model spectrum is compared in the inset of Fig. 2b with the model R_S/R_N spectrum evaluated with the same parameters in the bulk case (i.e., when $t \rightarrow \infty$). As noted above, the film spectrum is nearly constant for frequencies lower than the peak frequency of the bulk spectrum.

In discussing the fit results, we first remark that the Drude parameters Ω_i and γ_i are affected by rather large uncertainties (of the order of 20% when the uncertainty in the film thickness is considered) since these parameters are closely inter-related. However, the impact of these uncertainties is reduced in the total plasma frequency ($\Omega_{TOT} = \sqrt{\Omega_A^2 + \Omega_B^2} = 2.2 \pm 0.3 \text{ eV}$) and even more in $\sigma_0 = \sigma_{0A} + \sigma_{0B} = (7.0 \pm 0.5) 10^3 \Omega^{-1} \text{ cm}^{-1}$, corresponding to a residual resistivity $\rho_0 = 1/\sigma_0 = 0.140 \pm 0.015 \text{ m}\Omega \text{ cm}$, in good agreement with the measured value $\rho_0 = 0.15 \pm 0.01 \text{ m}\Omega \text{ cm}$ (see fig.1). This result supports the validity of the employed procedure. As to the gap values, we can safely pose $\Delta_A = 15.5 \pm 0.5 \text{ cm}^{-1}$ and $\Delta_B = 55 \pm 7 \text{ cm}^{-1}$. Indeed Δ_A is well determined since, as noted above, R_S/R_N is

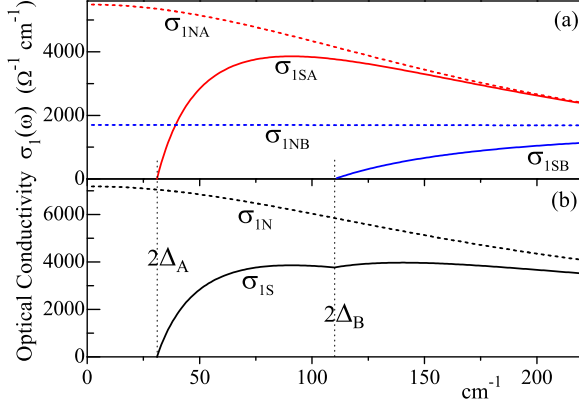


FIG. 3: (Color online) Contributions of A and B bands to σ_1 as evaluated by using the 2-b best fit parameter values in both the normal (N) and superconducting (S) state. (b) total σ_{1N} and σ_{1S} .

nearly constant below $2\Delta_A$, while the Δ_B value is much more uncertain since this gap does not give a clear spectral feature. Nonetheless, as discussed above, the B-band contribution needs to be included in the model in order to obtain a good description of the experimental R_S/R_N spectral shape.

We then attempted a two-band modelling of the $R(T)/R_N$ spectra measured at 12 and 18 K by using the 6 K values of the Drude parameters and using Δ_A and Δ_B as free parameters in the fitting procedure. As shown in Fig. 2b, it is not possible to obtain a satisfactory description of the measured spectra, in particular at low frequencies. As a consequence, the resulting Δ_A and Δ_B values are affected by large uncertainties, as shown in the inset of Fig. 2b where the normalized $\Delta(T)/\Delta_0$ values are reported, with $\Delta_0 = \Delta(6 \text{ K})$. In the same figure, the standard BCS $\Delta(T)/\Delta_0$ behaviour is reported for comparison. The poor agreement between the fit and the temperature-dependent data may indicate that the two-band model used here still provides an oversimplified description of the superconducting gap structure. Thus the possible presence of nodes in the gap or of a third gap of very low energy cannot be ruled out.

For a better understanding of the double-gap scenario, we consider in detail the frequency dependence of the optical conductivity σ_1 , as evaluated by using the best fit parameter values. The model σ_{1N} and σ_{1S} of the A- and B-band are reported separately in Fig. 3a up to 220 cm^{-1} , i.e. in the THz region where the effect of the superconducting gaps is dominant. In the normal state, since $\sigma_{0A} \approx 5500 \Omega^{-1} \text{ cm}^{-1}$ is roughly three times larger than σ_{0B} and γ_B is at least ten times larger than γ_A , the spectral shape of the total $\sigma_{1N} = \sigma_{1NA} + \sigma_{1NB}$ in the THz region is dominated by the A-band contribution, as shown in Fig. 3b. Our results are thus in agreement with

recent findings showing that the normal state conductivity of a number of 122 systems [30], and in particular of $\text{BaFe}_{2-x}\text{Co}_x\text{As}_2$ compounds [33], is given by a sharp component superimposed to a much broader component. In the superconducting state, since σ_{1SA} (σ_{1SB}) vanishes below $2\Delta_A$ ($2\Delta_B$), the total $\sigma_{1S} = \sigma_{1SA} + \sigma_{1SB}$ vanishes below the smaller optical gap $2\Delta_A$, as shown in Fig. 3b. Since, in general, R_S approaches 1 when σ_{1S} vanishes, this explains why only the effect of the smaller gap Δ_A is well evident in the R_S/R_N spectrum.

The gap values we obtained are compared in Table I with those reported in recent infrared/THz studies of $\text{BaFe}_{2-x}\text{Co}_x\text{As}_2$ samples. The reflectivity measurements of van Heumen *et al.* on a $x=0.14$ single crystal [28] provide evidence of a high-energy gap ($\Delta_B = 56 \text{ cm}^{-1}$) in very good agreement with our finding, while the low-energy gap value $\Delta_A = 26.5 \text{ cm}^{-1}$ is higher than our own value (15.5 cm^{-1}). Kim *et al.* [29] performed reflection and ellipsometry measurements on a $x=0.13$ single-crystal. According to their analysis, three isotropic gaps are necessary to obtain a good description of the experimental data. The low-energy gap Δ_A value is close to 25 cm^{-1} , while the two gaps at higher energy are around 40 and 78 cm^{-1} . Wu *et al.* [30] made reflectivity measurements on a $x=0.16$ crystal and their analysis provided evidence of a 25 cm^{-1} gap and also suggested the presence of a second gap at very low energy around 9 cm^{-1} . Gorshunov *et al.* [31], besides reflectance, performed transmittance measurements at very low frequencies on a film [17] with $x=0.2$, and found evidence of only one isotropic gap at 15 cm^{-1} , in very good agreement with our Δ_A value. THz conductivity spectroscopy measurements by Nakamura *et al.* [32] on a $x=0.2$ film showed the presence of a gap at 22.4 cm^{-1} . The reflectivity measurements of Nakajima *et al.* [33] on single crystals gave evidence of a single gap at 40 cm^{-1} for $x=0.12$, around 25 cm^{-1} for $x=0.16$. Finally, Fisher *et al.* [34] measured the complex dynamical conductivity of a $x=0.2$ film and their analysis gave a nodeless gap at 24 cm^{-1} and a nodal gap around 64 cm^{-1} .

Several different measurements therefore indicate a low energy gap Δ_A mostly between 15 and 25 cm^{-1} , as reported in Table I. In trying to explain this uncertainty, it might be necessary to consider various effects, such as disorder [4, 12, 21, 22] and doping level [8] which can differently affect the various samples, and, in the case of films, the strain imposed by the substrate [17]. Furthermore, in the case of standard reflectance measurements, it is important to keep in mind that, in terms of signal to noise ratio, the quality of THz measurements on a large surface film can be better than that of measurements on crystals, especially when the wavelength approaches the crystal size. The difference among the observed Δ_A values might then be explained, but more bothersome is the disagreement in the number and values of the high-energy gaps, as summarized in Table I.

TABLE I: THz supeconductings gaps in $\text{BaFe}_{2-x}\text{Co}_x\text{As}_2$ compounds from the present work and literature [28–34].

	Present work	Ref. [28]	Ref. [29]	Ref. [30] ^a	Ref. [31]	Ref. [32] ^b	Ref. [33]	Ref. [33]	Ref.[34]
Co-doping	0.16	0.14	0.13	0.16	0.2	0.2	0.12	0.16	0.2
T_c (K)	22.5	23	24.5	25	20	19.9	25	20	25
N. of gaps	2	2	3	2	1	1	1	1	2
Δ_A (cm^{-1})	15.5	26.5	25	25	15	22.4	40	25	24
Δ_B (cm^{-1})	55	56	40	-	-	-	-	-	64
Δ_C (cm^{-1})	-	-	78	-	-	-	-	-	-

^a The authors suggest the presence of a low energy gap around 9 cm^{-1} , below the range in which reliable data could be acquired.

^b The authors do not exclude an high energy gap since their measurements are performed up to 1 THz (33 cm^{-1}).

IV. CONCLUSIONS

We measured the THz reflectance properties of a high quality epitaxial film of $\text{BaFe}_{1.84}\text{Co}_{0.16}\text{As}_2$ with $T_c=22.5 \text{ K}$ by measuring the $R(T)/R_N$ spectrum, i.e. the reflectivity ratio between the superconducting state (for $6 \leq T \leq 22 \text{ K}$) and the 25 K (normal state) reflectance. The measured R_S/R_N spectrum (with $R_S = R(6 \text{ K})$) first suggests the presence of a superconducting gap Δ_A close to 15 cm^{-1} . We find that only a two-band model, with a gap opening in both bands, can describe the measured R_S/R_N spectrum, and in particular its smoothly decreasing slope. The low-energy Δ_A gap ($\Delta_A=15.5 \pm 0.5 \text{ cm}^{-1}$) and the high-energy gap Δ_B ($\Delta_B=55 \pm 7 \text{ cm}^{-1}$) correspond to $2\Delta/kT_c$ values close to 2 and 7, respectively. The R_S/R_N data are thus compatible with a two-band scenario, with a nodeless isotropic gap opening in both bands. Nevertheless, the poor agreement between the model and experimental $R(T)/R_N$ at 12 and 18 K can be interpreted as an indication for ungapped states at low energies. Their presence may be attributed either to nodes or to the presence of gaps at energies so low as to get thermally excited carriers at relatively modest temperatures.

Despite some differences, the magnitude of the low-energy optical gap recently found by different groups sub-

stantially agree with our Δ_A value, but there is a large disparity on the reported number of gaps and on their values. In order to resolve this important issue, THz transmission measurements on $\text{BaFe}_{2-x}\text{Co}_x\text{As}_2$ films, to be performed in the entire THz region where gap effects are expected, could be of great help in settling this debate. Indeed, in a multigap superconductor, transmittance measurements are more sensitive to the features related to the high-energy gap(s), while reflectance is more dependent on the low-energy one, as we have shown in the V_3Si case [38].

Acknowledgements

Work at NHMFL was supported under NSF Cooperative Agreement DMR-0084173, by the State of Florida, and by AFOSR grant FA9550-06-1-0474. Work at the University of Wisconsin was supported by the US Department of Energy, Division of Materials Science, under Award No. DE-FG02-06ER463. The authors thank M.S. Rzhowski for helpful discussion. Work at the University of Rome was partially funded by CARIPLO Foundation (Project 2009-2540 "Chemical Control and Doping Effects in Pnictide High-temperature Superconductors"), at the University of Genova by the "Italian Foreign Affairs Ministry (MAE) - General Direction for the Cultural Promotion".

-
- [1] Kamihara Y., Watanabe T., Hirano M. and Hosono H., J. Am. Chem. Soc. **130**, (2008) 3296
 - [2] Qazilbash M.M., Hamlin J.J., Baumbach R.E., Lijun Zhang, Singh D.J., Maple M.B. and Basov D.N., Nature Physics **5**, (2009) 647
 - [3] Yang W.L., Sorini A.P., Chen C-C., Moritz B., Lee W.-S., Vernay F., Olalde-Velasco P., Denlinger J.D., Delley B., Chu J.-H., Analytis J.G., Fisher I.R., Ren Z.A., Yang J., Lu W., Zhao Z.X., van den Brink J., Hussain Z., Shen Z.-X. and Devereaux T.P., Phys. Rev. B **80**, (2009) 014508
 - [4] Muschler B., Prestel W., Hackl R., Devereaux T.P., Analytis J.G., Jiun-Haw Chu and Fisher I.R., Phys. Rev. B **80**, (2009) 180510(R)
 - [5] Goko T., Aczel A.A., Baggio-Saitovitch E., Bud'ko S.L., Canfield P.C., Carlo J.P., Chen G.F., Dai P., Hamann A.C., Hu W.Z., Kageyama H., Luke G.M., Luo J.L., Nachumi B., Ni N., Reznik D., Sanchez-Candela D.R., Savici A.T., Sikes K.J., Wang N.L., Wiebe C.R., Williams T.J., Yamamoto T., Yu W. and Uemura Y.J., Phys. Rev. B **80**, (2009) 024508
 - [6] Salem-Sugui Jr. S., Ghivelder L., Alvarenga A.D., Pimentel Fr. J.L., Luo H., Wang Z. and Wen H.H., Phys. Rev. B **80**, (2009) 014518
 - [7] Gordon R.T., Ni N., Martin C., Tanatar M.A., Vannette M.D., Kim H., Samolyuk G.D., Schmalian J., Nandi S., Kreyssig A., Goldman A.I., Yan J.Q., Bud'ko S.L., Canfield P.C., Prozorov R., Phys. Rev. Lett. **102**, (2009)

- 127004
- [8] Terashima K., Sekiba Y., Bowen J. H., Nakayama K., Kawahara T., Sato T., Richard P., Xu Y.-M., Li L. J., Cao G. H., Xug Z.-A., Ding H. and Takahashi T., *Proc. Natl. Acad. Sci.* **106**, (2009) 7330
 - [9] Samuely P., Pribulova Z., Szabo P., Pristas G., Budko S.L. and Canfield P.C., *Physica C* **469**, (2009) 507
 - [10] Williams T.J., Aczel A.A., Baggio-Saitovitch E., Bud'ko S.L., Canfield P.C., Carlo J.P., Goko T., Munevar J., Ni N., Uemura Y.J., Yu W. and Luke G.M., *Phys. Rev. B* **80**, (2009) 094501
 - [11] Hardy F., Wolf T., Fisher R.A., Eder R., Schweiss P., Adelman P., v. Löhneysen H. and Meingast C., *Phys. Rev. B* **81**, (2010) 0060501
 - [12] Tanatar M.A., Reid J.P., Shakeripour H., Luo X.G., Doiron-Leyraud N., Ni N., Bud'ko S.L., Canfield P.C., Prozorov R. and Taillefer L., *Phys. Rev. Lett.* **104**, (2010) 067002
 - [13] Luan L., Auslaender O.M., Lippman T.M., Hicks C.W., Kalisjy B., Chu J.H., Alalytis J.G., Fisher I.R., Kirtley J.R. and Moler K.A., *Phys. Rev. B* **81**, (2010) 100501
 - [14] Mazin I.I., Singh D.J., Johannes M.D. and Du M.H., *Phys. Rev. Lett.* **101**, (2008) 057003
 - [15] Luo H., Wang Z., Yang H., Cheng P., Zhu X. and Wen H.H. *Supercond. Sci. Technol.* **21**, (2008) 125014
 - [16] Lee S., Jiang J., Nelson C.T., Bark C.W., Weiss J.D., Tarantini C., Jang H.W., Folkman C.M., Baek S.H., Polyanskii A., Abrahimov D., Yamamoto A., Zhang Y., Pan X.Q., Hellstrom E.E., Larbalestier D.C. and Eom C.B. *Nature Materials* **9**, (2010) 397
 - [17] Iida K., Hänisch J., Hünhe R., Kurth F., Kidszun M., Haindl S., Werner J., Schultz L. and Holzapfel B., *Appl. Phys. Lett.* **95**, (2009) 192501
 - [18] Sefat A.S., Jin R., McGuire M.A., Sales B.C., Singh D.J. and Mandrus D., *Phys. Rev. Lett.* **101**, (2008) 117004
 - [19] Yin Y., Zech M., Williams T.L., Wang X.F., Wu G., Chen X.H. and Hoffman J.E. *Phys. Rev. Lett.* **102**, (2009) 097002
 - [20] Massee F., Huang Y., Huisman R., de Jong S., Goedkoop J.B. and Golden M.S., *Phys. Rev. B* **79**, (2009) 220517(R)
 - [21] Hashimoto K., Shibauchi T., Kasahara S., Ikada K., Tonegawa S., Kato T., Okazaki R., van der Beek C.J., Konczykowski M., Takeya H., Hirata K., Terashima T. and Matsuda Y., *Phys. Rev. Lett.* **102**, (2009) 207001
 - [22] Carbotte J. P. and Schachinger E. *Phys. Rev. B* **81**, (2010) 104510
 - [23] Burns G. *Solid state physics* (Academic Press, Boston, 1990)
 - [24] Mattis D.C. and Bardeen J., *Phys. Rev.* **111**, (1958) 412
 - [25] Tinkham M. *Introduction to Superconductivity* (McGraw-Hill, New York, 1975)
 - [26] Hu W.Z., Zhang Q.M. and Wang N.L. *Physica C* **469**, (2009) 545
 - [27] Drechsler S.L., Rosner H., Grobosch M., Behr G., Roth F., Fuchs G., Koepf K., Schuster R., Malek J., El-gazzar S., Rotter M., Johrendt D., Klauss H.H., Büchner B. and Knupfer M. arXiv:0904.0827 preprint, 2009
 - [28] van Heumen E., Huang Y., de Jong S., Kuzmenko A.B., Golden M.S. and van der Marel D., arXiv:0912.0636 preprint, 2009
 - [29] Kim K.W., Rössle M., Dubroka A., Malik V.K., Wolf T. and C. Bernhard, arXiv:0912.0140 preprint, 2009
 - [30] Wu D., Barisic N., Kallina P., Faridian A., Gorshunov B., Drichko N., Li L.J., Lin X., Cao G.H., Xu Z.A., Wang N.L. and Dressel M., *Phys. Rev. B* **81**, (2010) 100512(R)
 - [31] Gorshunov B., Wu D., Voronkov A.A., Kallina P., Iida K., Haindl S., Kurth F., Schultz L., Holzapfel B. and Dressel M., *Phys. Rev. B*, **81** (2010) 060509(R)
 - [32] Nakamura D., Imai Y., Maeda A., Katase T., Hiramatsu H., and Hosono H., arXiv:0912.4351v2 preprint, 2010
 - [33] Nakajima M., Ishida S., Kihou K., Tomioka Y., Ito T., Yoshida Y., Lee C. H., Kito H., Iyo A., Eisaki H., Kojima K. M., and Uchida S., *Phys. Rev. B* **81**, (2010) 104528
 - [34] Fischer T., Pronin A. V., Wosnitza J., Iida K., Kurth F., Haindl S., Schultz L., Holzapfel B., and Schachinger E., arXiv:1005.0692v1 preprint, 2010.
 - [35] Lupi S., Nucara A., Perucchi A., Calvani P., Ortolani M., Quaroni L. and Kiskinova M., *J. Opt. Soc. Am. B* **24**, (2007) 959
 - [36] Ortolani M., Dore P., Di Castro D., Perucchi A., Lupi S., Ferrando V., Putti M., Pallecchi I., Ferdeghini C. and Xi X.X., *Phys. Rev. B* **77**, (2008) 100507(R)
 - [37] Kuzmenko A.B., *Phys. C* **456**, (2007) 63
 - [38] Perucchi A., Nicoletti D., Ortolani M., Marini C., Sopracase R., Lupi S., Schade U., Putti M., Pallecchi I., Tarantini C., Ferretti M., Ferdeghini C., Monni M., Bernardini F., Massidda S. and Dore P., *Phys. Rev. B* **81**, (2010) 092509
 - [39] Zimmermann W., Brandt E.H., Bauer M., Seider E. and Genzel L., *Phys. C* **183**, (1991) 99
 - [40] Dressel M. and Grüner G., *Electrodynamics of Solids* (Cambridge University Press, Cambridge, England, 2002)
 - [41] Dore P., Paolone A., and Trippetti R., *J. Appl. Phys.* **80**, (1996) 5270; Dore P., De Marzi G. and Paolone A., *Int. J. of ir and mm Waves* **18**, (1997) 125